Materials and Methods

In silico screening of peptide hormone candidates

We arranged TAIR 10 annotated *Arabidopsis* proteins (35,176 ORFs) as a function of sequence length as described previously (*10*), and retrieved 1,690 ORFs encoding proteins with lengths ranging from 50 to 150 amino acids. Predicted peptides and small proteins were screened for the presence of predicted N-terminal signal peptides that would direct them to the secretory pathway, using the HMM version of the SignalP 3.0 server. This reduced the number of ORFs to 1,086 when we set the threshold value of signal peptide probability to >0.75. We further excluded ORFs encoding peptides containing six or more Cys residues that could form intramolecular disulfide bonds. The resulting 465 cysteine-poor ORFs included 204 ORFs encoding peptides of unknown function. These 204 peptides were subjected to WU BLAST 2.0 database analysis to search for homologous peptides containing a conserved domain in the C-terminal region.

Peptide structure analysis

For the peptide structure analysis, a cDNA of *At2g16385* (*CIF1*) was obtained by RT-PCR using total RNA isolated from *Arabidopsis* roots using the specific primers (Table S1). The resulting fragment was cloned into the *Xho*I/*Spe*I-digested estradiol-inducible binary vector pER8 (*17*) using In-Fusion HD cloning kit (Clontech). The constructs were introduced into wild-type Columbia by *Agrobacterium*-mediated transformation. *Arabidopsis* seeds (≈100 seeds) containing the estradiol-inducible *At2g16385* (*CIF1*) gene were sown directly in 100 ml of B5 liquid medium containing 1.0% sucrose and incubated without shaking under continuous light at 22°C. After 14 days of culture, expression of the transgene was induced by addition of 75 μM estradiol for 24 h. Extraction of peptides from culture medium by *o*-chlorophenol was performed as described previously (*10*). Fractions containing total secreted peptide were dissolved in 500 μl of 0.1% TFA. Nano LC-MS analysis was performed using a DiNa-M splitless nano HPLC system (KYA Technologies, Japan) connected to an LTQ Orbitrap XL mass spectrometer (Thermo Scientific). Aliquots of peptide fractions (5 μl) were loaded onto a C_{18} trap column (0.5 mm i.d. × 1 mm cartridge; KYA Technologies) and washed with 10 μl of 0.1% formic acid. Peptides were subsequently eluted from the precolumn and separated on a MonoCap C_{18} Fast-flow nano-column (100 μm i.d. × 150 mm; GL Sciences) using a gradient of 2-50% acetonitrile containing 0.1% formic acid for 30 min at a flow rate of 500 nl/min. Tandem mass spectra were obtained by scanning the mass range from *m*/*z* 400 to *m*/*z* 2,000 using data-dependent acquisition methods with HCD fragmentation. The data were analyzed with Proteome Discoverer 1.3 software using the SEQUEST search engine (Thermo Scientific).

Peptide synthesis

CIF1 and CIF2 were chemically synthesized by Fmoc solid-phase chemistry using an automated peptide synthesizer (Biotage Initiator^{+} Alstra) on TrtA-PEG resin. For peptide treatment, CIF peptides were added to the medium at 100 nM, unless otherwise stated.

Synthesis of photoactivatable [^{125}I]ASA-CIF1

The photoactivatable and radiolabeled CIF1 analogue [^{125}I]ASA-CIF1 was prepared basically according to a previous report (*18*). The Fmoc-protected CIF1 analogue Fmoc-[Lys^{11}]CIF1 was synthesized via Fmoc chemistry using a peptide synthesizer. Lys(Dde) was incorporated into Lys^{17} to prevent side reactions. 4-Azidosalicylic acid succinimidyl ester (0.9 mg, Pearce), Fmoc-[Lys^{11}]CIF1 (3.6 mg), and $NaHCO_3$ (1.0 mg) were dissolved in 200 µl of 50% acetonitrile and stirred for 1 h in the dark at room temperature. Crude peptides were purified by reverse-phase HPLC and lyophilized to yield Fmoc-[(4-azidosalicyl)Lys^{11}]CIF1. The Dde and Fmoc groups were deprotected by treatment with 2% hydrazine in 200 µl of 50% acetonitrile for 1 h, followed by addition of 100 µl of piperidine with incubation for 1 h. The deprotected peptide was purified by reverse-phase HPLC and lyophilized to obtain [(4-azidosalicyl)Lys^{11}]CIF1 (ASA-CIF1). ASA-CIF1 was further radioiodinated using the chloramine T method. The labeled peptide was purified by reverse-phase HPLC to yield analytically pure [^{125}I]ASA-CIF1 at a specific radioactivity of 90 Ci/mmol.

Photoaffinity labeling using an *Arabidopsis* receptor kinase expression library

Preparation of the *Arabidopsis* receptor kinase expression library was reported previously (*19*). Photoaffinity labeling and immunoprecipitation were performed according to previous reports (*18-20*) using 30 nM [^{125}I]ASA-CIF1. For the competitive binding assay, 300-fold molar excesses of unlabeled CIF1 and CIF2 peptides were used.

T-DNA-tagged mutants

T-DNA-tagged *cif* and *gso* mutants were identified in the SALK and FLAG T-DNA collections (*cif1-1*, SALK_105801; *cif2-1*, FLAG_270C08; *gso1-2*, SALK_103965; *gso2-2*, SALK_143123). The location of the T-DNA insertion and the homozygosity of the mutation were confirmed by genomic PCR and RT-PCR. *Arabidopsis* plants were grown on modified half-strength MS medium as previously described (*21*), with 0.7% agar for phenotypic and microscopic analyses. All plants were grown under continuous light at 22°C.

Promoter analysis

To analyze the promoter activities of *CIF1* and *CIF2*, we amplified the upstream 2.5-kb promoter regions of the *CIF* genes using genomic PCR and cloned them by translational fusion in frame with the β-glucuronidase (GUS) coding sequence in the *Xba*I/*Sma*I-digested binary vector pBI101 using NEBuilder HiFi DNA Assembly Kit (New England BioLabs). GUS activity was assessed visually by according to a conventional protocol, with X-Gluc as the substrate.

Complementation analysis

For complementation analysis, the full-length *CIF2* genomic fragment containing the 2.5-kb promoter region was cloned into the *Xba*I/*Sac*I-digested binary vector pBI101-Hm using NEBuilder HiFi DNA Assembly Kit. The constructs were introduced into the *cif1-1 cif2-1* double mutant by *Agrobacterium*-mediated transformation.

Observation of the Casparian strip

For analysis of apoplastic barrier loss, roots of 10-day-old seedlings were incubated for 10 min in a fresh solution of 15 μM propidium iodide (PI) and rinsed twice with water, as previously described (*22*, *23*). The roots were then observed under a confocal laser-scanning microscope (Olympus FV300) equipped with a helium-neon laser and excitation at 543 nm. To visualize the Casparian strip, roots of 10-day-old seedlings were cleared as previously described (*24*), and autofluorescence of the Casparian strip was visualized by argon laser excitation at 488 nm. For quantitative analysis of discontinuous Casparian strips, the number of holes in the Casparian strips was determined as previously described (*5*). To visualize the Casparian strip domain using CASP1-GFP, we amplified both the genomic fragment of the *CASP1* gene including the 2.0-kb 5'-upstream region and the cDNA fragment of GFP using PCR. These two fragments were cloned by translational fusion using three-component ligation into the *Xba*I/*Sac*I-digested binary vector pBI101-Hm using In-Fusion HD cloning kit. The constructs were introduced into the *cif1-1 cif2-1* double mutant by *Agrobacterium*-mediated transformation. GFP signals were observed under a confocal laser-scanning microscope with argon laser excitation at 488 nm.

Toluidine blue test

For analysis of loss of the cuticle, 7-day-old seedlings were incubated for 5 min in a fresh solution of 0.05% toluidine blue, rinsed twice with water, and observed under a stereo microscope (Olympus SZX16).

Examination of the effects of excess mineral ions and low pH

For excess iron treatment, the concentration of Fe(III)-EDTA in the culture medium was increased to 300 or 500 μM. For excess manganese and zinc treatment, the concentration of $MnCl_2$ or $ZnCl_2$ was increased to 500 or 200 μM, respectively. For excess copper treatment, the concentration of $CuCl_2$ was increased to 5 μM. MES buffer (2.5 mM) was used for evaluating the effect of pH 5.5, and citrate buffer (2.5 mM) was used to evaluate the effect of pH 4.5.

Quantitative RT-PCR

Total RNA was prepared from roots using an RNeasy kit (Qiagen). First-strand cDNA was synthesized from 2 μg of root-derived total RNA using the Superscript III first strand synthesis system for RT-PCR (Invitrogen) according to the manufacturer's protocol. Primers and Taqman probes were designed using Probe Finder software in the Universal Probe Library (UPL) Assay Design Center (Roche Applied Science, Germany). All PCR reactions were performed using a StepOne System (Applied Biosystems). Constitutively expressed *EF-1α* was used as a reference gene for normalization of quantitative RT-PCR data.

Synchrotron radiation X-ray fluorescence spectrometry of xylem sap

Fifteen-day-old *Arabidopsis* seedlings grown vertically on modified MS agar medium (1.5% agar) were transferred to MS agar medium (0.7% agar) containing 300 or 500 μM iron. After 3 h of horizontal incubation, the hypocotyl of each seedling was cut below the cotyledons and a short length (≈10 mm) of 0.5-mm-diameter silicon tubing was placed over the hypocotyl stump. Xylem sap was collected in the silicon tubing for 12 h

and recovered in a microtube by centrifugation. We obtained up to ≈20 μl of xylem sap from 24 *Arabidopsis* seedlings. The amount of Fe in 10 μl of xylem sap or culture medium was directly analyzed by synchrotron radiation X-ray fluorescence spectrometry using a hard X-ray beamline BL5S1 at 12 keV for 300 sec by using a silicon drift detector in the Aichi Synchrotron Radiation Center.

Ion chromatography of xylem sap

The amount of potassium in the xylem sap was analyzed by ion chromatography using a Dionex ICS-1500 series ion chromatograph equipped with a conductivity detector. Aliquots (25 μl) of 1:100 diluted xylem sap or culture medium were separated on a Dionex IonPac CS12A column (4 mm i.d. × 250 mm) with 20 mM methanesulfonic acid for 15 min at a flow rate of 1 ml/min.

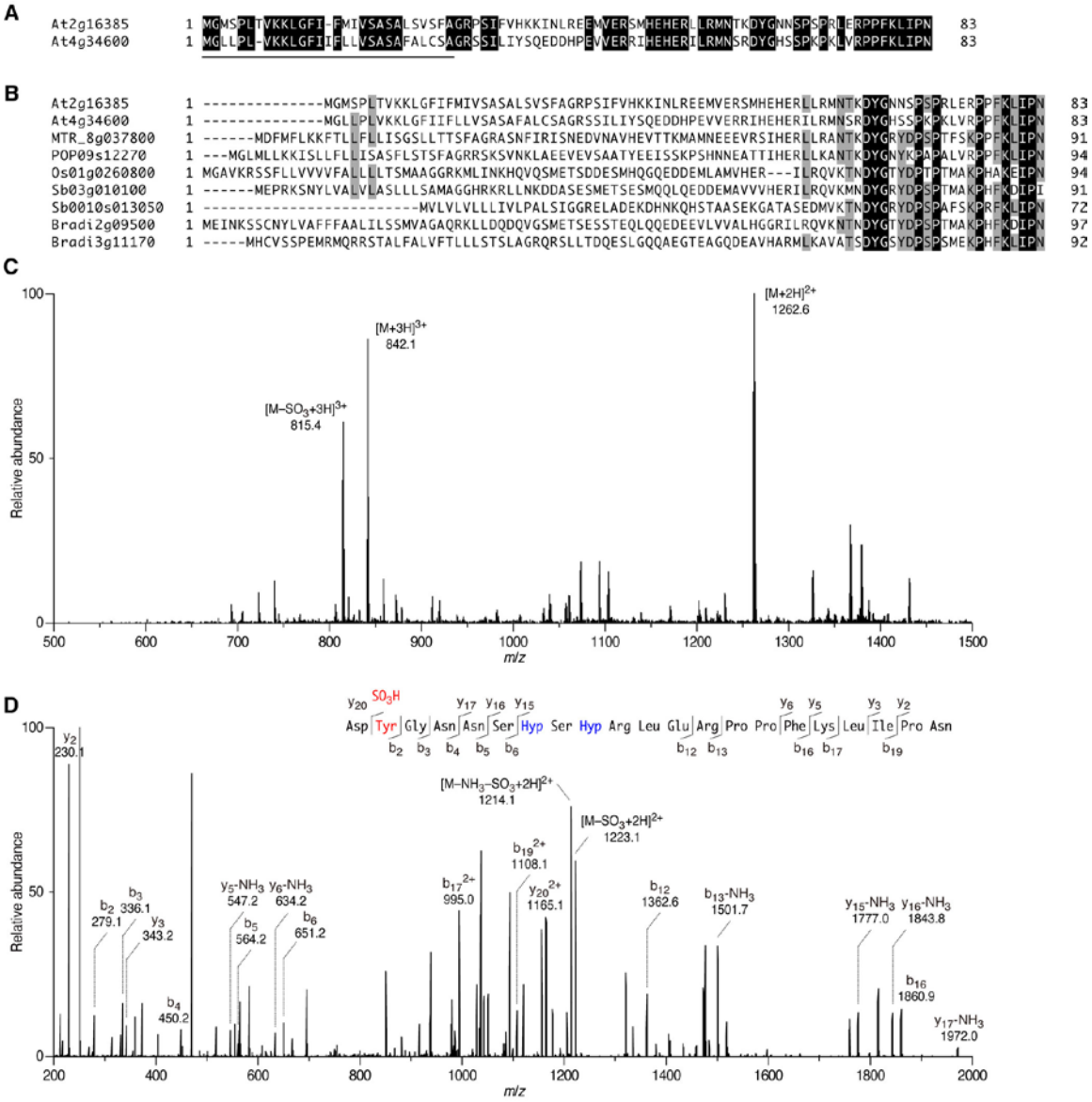

Fig. S1.

Analysis of the At2g16385 and At4g34600 peptides. (**A**) Sequence alignment of At2g16385 and At4g34600. The putative signal peptide is underlined. The residues conserved in both peptides are shaded in black. (**B**) Multiple sequence alignment of At2g16385-family peptides in several representative land plants. The residues conserved in all proteins are shaded in black, and similar residues are shaded in gray. (**C**) Nano LC-MS spectrum of the mature At2g16385 peptide detected in the culture medium of *Arabidopsis* plants overexpressing At2g16385 (CIF1). (**D**) Nano LC-MS/MS spectrum of the mature At2g16385 (CIF1) peptide. The MS/MS spectrum of the precursor ion at *m*/*z* 1262.6 in (C) indicated that At2g16385 is a 21-residue tyrosine-sulfated peptide.

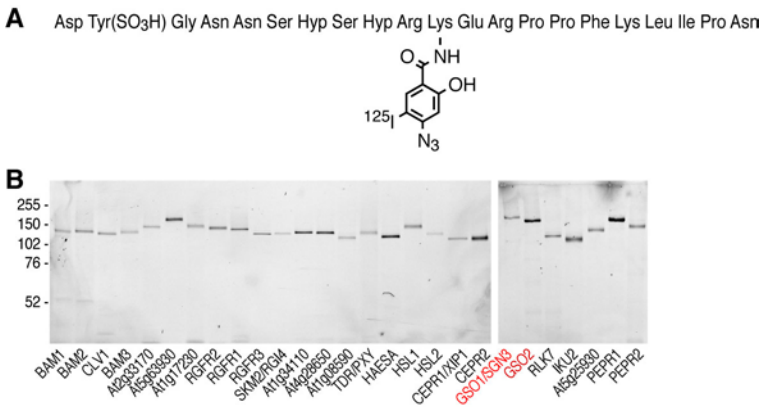

Fig. S2

Photoaffinity labeling using [^{125}I]ASA-At2g16385 against a receptor kinase expression library. (**A**) Structure of [^{125}I]ASA-At2g16385 ([^{125}I]ASA-CIF1), in which photoactivatable 4-azidosalicylic acid (ASA) is incorporated into the 11th residue from the N-terminus. (**B**) The loading control of HaloTag-fused receptor kinase proteins for Figure 1C, visualized using HaloTag TMR.

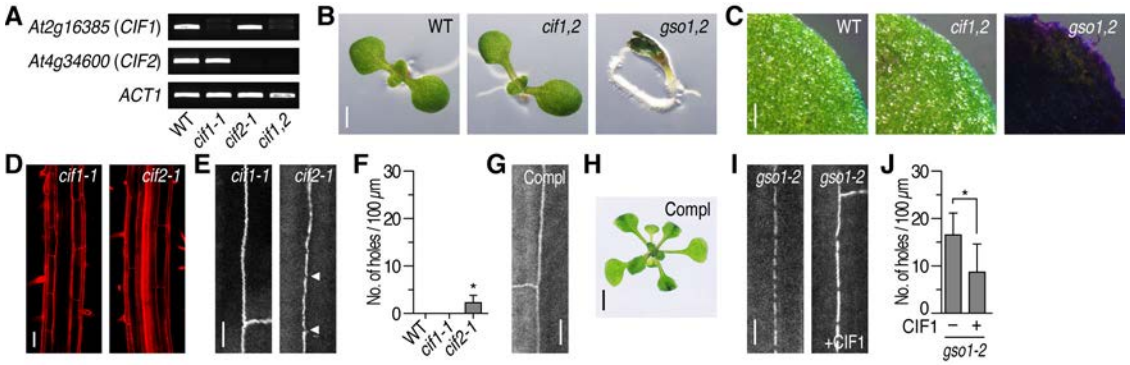

Fig. S3

Analysis of T-DNA insertion mutants of the *At2g16385* and *At4g34600* genes. (**A**) RT-PCR confirmed the absence of full-length transcripts in the roots of corresponding mutants. (**B**) Seven-day-old seedlings of the At2g16385 At4g34600 ligand double mutant (*cif1,2*) and *gso1/sgn3 gso2* double mutant (*gso1,2*). (**C**) Toluidine blue permeability of the cotyledon cuticle of the mutants. (**D**) PI penetration into the vasculature in the single mutants. (**E**) Casparian strip in the single mutants visualized by autofluorescence. (**F**) Quantitative analysis of the number of holes in the Casparian strips shown in (E). (**G**) Casparian strip in *cif1-1 cif2-1* mutant complemented with the *CIF2* gene. (**H**) Two-week-old plants of the complemented line. (**I**) Casparian strip in the *gso1-2* single mutant in the absence or presence of 100 nM CIF1 peptide. (**J**) Quantitative analysis of the number of holes in the Casparian strips shown in (I). Scale bar: (B) 1 mm; (C) 50 µm; (D, E, G, I) 10 µm; (H) 5 mm.

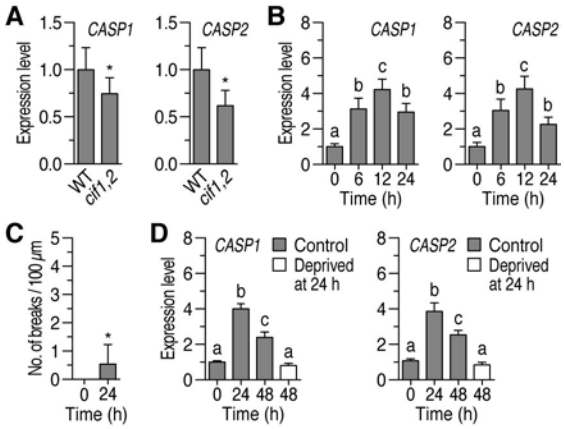

Fig. S4

Expression levels of *CASP1* and *CASP2* in the *cif1-1 cif2-1* double mutant. (**A**) qRT-PCR analysis of *CASP1* and *CASP2* in wild-type and double mutant plants (n = 6). (**B**) Changes in levels of *CASP1* and *CASP2* transcripts in the double mutant after treatment with 100 nM CIF1 peptide (n = 6). (**C**) Quantitative analysis of the number of breaks shown in Figure 3J (n = 11). (**D**) Changes in levels of *CASP1* and *CASP2* transcripts in the double mutant after CIF1 peptide treatment and deprivation (n = 3). Double mutant that had been treated with CIF1 peptide for 24 h was transferred to fresh medium devoid of the peptide (n = 3).

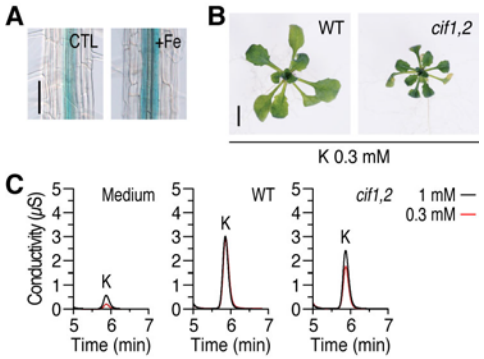

Fig. S5

Response of the *cif1-1 cif2-1* double mutant under various ion conditions. (**A**) Promoter activity of *CIF1* in roots treated with 75 µM iron at pH 5.5 as a control or 500 µM iron at pH 4.5 for 24 h. (**B**) Growth of the wild-type and mutant plants under low potassium conditions (0.3 mM) for 7 days. (**C**) Comparison of potassium levels between the culture medium, the wild-type xylem sap, and the mutant xylem sap using ion chromatography. Scale bar: (A) 100 µm; (B) 5 mm.

Table S1

List of primers used in this study. The adaptor sequence is underlined.

Experiment		Sequence (5'-3')
CIF1 expression in pER8	Forward	CGACTCTAGCCTCGACCAAGGAGAGATAA
	Reverse	CTAGTCGATCCAGGCGGATGGATTAGAACC
CIF2 complementation in pBI101-Hm	Forward	GCCTGCAGGTCGACTTTATGTATAATCATCTCC
	Reverse	ATCGGGGAAATTCGAGCTGTCTGGCATCTATATA
CIF1 promoter GUS in pBI101	Forward	GCCTGCAGGTCGACTCCATCCTTTACCGAAC
	Reverse	AGGGACTGACCACCCATAACTTAATTATCTCTC
CIF2 promoter GUS in pBI101	Forward	GCCTGCAGGTCGACTGGTCAAAATTCTAATCTTTC
	Reverse	AGGGACTGACCACCCCTTTCTCCTTTCAAT
cif1-1 T-DNA mutant screening	Forward	TTCCAAGGAGAGATAATTAAGTTATG
	Reverse	GGATGGATTAGAACCAATTCTAATG
cif2-1 T-DNA mutant screening	Forward	ATACACAAGATACAGCTTAAGGCACATC
	Reverse	GTCTGGCATCTATATATAGTCGATCGG
CASP1 for CASP1-GFP in pBI101-Hm	Forward	GCAGGTCGACTCTAGATGAGAATTGGCGATTAAAG
	Reverse	GCCCTTGCTCACCATATGCCTCTTGAGGGCGAT
GFP for CASP1-GFP in pBI101-Hm	Forward	ATGGTGAGCAAGGGCGAGGA
	Reverse	GATCGGGGAAATTCGCGCTTTACTTGTACAGCTCGTC
CIF1 RT-PCR	Forward	TTCCAAGGAGAGATAATTAAGTTATG
	Reverse	GGATGGATTAGAACCAATTCTAATG
CIF2 RT-PCR	Forward	ATACACAAGATACAGCTTAAGGCACATC
	Reverse	GTCTGGCATCTATATATAGTCGATCGG
ACT1 RT-PCR	Forward	GACAGCCAAAACCAGCTCATC
	Reverse	CGATGGACCTGACTCGTCATAC
CIF1 qRT-PCR	Forward	CGACCATCGATTTTTGTTCAT
	Reverse	TCTTAGAAGCCTCTCATGCTCA
CIF2 qRT-PCR	Forward	GTTCTGCAGGCCGATCAT
	Reverse	TTCTCAGAATTCTCTCATGCTCA
CASP1 qRT-PCR	Forward	AGTTCCAAGCCGGTTACGAT
	Reverse	CGACTACGGCTACGGCTATC
CASP2 qRT-PCR	Forward	TTGCTCGTTCTTGACACTGG
	Reverse	GTCTCCAAACTGTTGGCAAAT
EF-1α qRT-PCR	Forward	CTTGGTGTCAAGCAGATGATTT
	Reverse	CGTACCTAGCCTTGGAGTATTTG

References

17. J. Zuo, Q. W. Niu, N. H. Chua, *Plant J* **24**, 265-273 (2000).
18. M. Ogawa, H. Shinohara, Y. Sakagami, Y. Matsubayashi, *Science* **319**, 294 (2008).
19. H. Shinohara, A. Mori, N. Yasue, K. Sumida, Y. Matsubayashi, *Proc Natl Acad Sci U S A*, (2016).
20. R. Tabata *et al.*, *Science* **346**, 343-346 (2014).
21. B. D. Gruber, R. F. Giehl, S. Friedel, N. von Wiren, *Plant Physiol* **163**, 161-179 (2013).
22. J. Alassimone, S. Naseer, N. Geldner, *Proc Natl Acad Sci U S A* **107**, 5214-5219 (2010).
23. S. Naseer *et al.*, *Proc Natl Acad Sci U S A* **109**, 10101-10106 (2012).
24. J. E. Malamy, P. N. Benfey, *Development* **124**, 33-44 (1997).